An improved algorithm for reaction path following

Carlos Gonzalez and H. Bernhard Schlegel[a)]
Department of Chemistry, Wayne State University, Detroit, Michigan 48202

(Received 16 June 1988; accepted 12 October 1988)

A new algorithm is presented for obtaining points on a steepest descent path from the transition state of the reactants and products. In mass-weighted coordinates, this path corresponds to the intrinsic reaction coordinate. Points on the reaction path are found by constrained optimizations involving all internal degrees of freedom of the molecule. The points are optimized so that the segment of the reaction path between any two adjacent points is given by an arc of a circle, and so that the gradient at each point is tangent to the path. Only the transition vector and the energy gradients are needed to construct the path. The resulting path is continuous, differentiable and piecewise quadratic. In the limit of small step size, the present algorithm is shown to take a step with the correct tangent vector and curvature vector; hence, it is a second order algorithm. The method has been tested on the following reactions: $HCN \rightarrow CNH$, $SiH_2 + H_2 \rightarrow SiH_4$, $CH_4 + H \rightarrow CH_3 + H_2$, $F^- + CH_3F \rightarrow FCH_3 + F^-$, and $C_2H_5F \rightarrow C_2H_4 + HF$. Reaction paths calculated with a step size of 0.4 a.u. are almost identical to those computed with a step size of 0.1 a.u. or smaller.

I. INTRODUCTION

For some reactions, the energy surface can be rather complicated. It may not be immediately obvious from either the structure of the transition state or the orientation of the transition vector whether the transition state connects the desired reactants and products. In such cases it may be necessary to follow the reaction path[1] part of the way from the transition state to the reactants and/or the products. For other reactions, it may be desirable to compute a portion of the energy surface along the reaction path near the transition structure, so that the kinetics can be treated by variational transition state theory[2] or by reaction path Hamiltonian methods.[3] In either case, an efficient and accurate method is needed to follow the reaction path.

In any given coordinate system, a reaction path can be defined as the steepest descent path or minimum energy path (MEP) from the transition state down to the reactants and down to the products. If mass-weighted Cartesian coordinates are used, this path is the intrinsic reaction coordinate (IRC).[1] Several approaches have been developed to follow reaction paths,[4–9] but most algorithms find tightly curved reaction paths difficult to follow and require small step sizes to be used.

A new reaction path-following algorithm is proposed that can follow curved reaction paths with comparatively large step sizes and does not require the calculation of the Hessian at points along the path. The algorithm is well suited for molecular orbital calculations, where the energy and gradient calculations are costly and must be kept to a minimum. The method has been tested on a two-dimensional model potential,[6] and has been applied to a few simple chemical reactions: $HCN \rightarrow HNC$, $SiH_2 + H_2 \rightarrow SiH_4$, $CH_4 + H \rightarrow CH_3 + H_2$, $F^- + CH_3F \rightarrow FCH_3 + F^-$, and $C_2H_5F \rightarrow C_2H_4 + HF$.

II. THEORY

The simplest method of following a reaction path is to solve the differential equation for the intrinsic reaction path[1]:

$$d\mathbf{x}^{\mathrm{IRC}}/ds = \mathbf{g}_k/|\mathbf{g}_k|, \tag{1}$$

where $\mathbf{g}$ is the gradient in mass weighted Cartesian coordinates. As a first approximation to the solution of Eq. (1), a series of small linear steps can be taken in the descent direction[8,9] such that

$$\Delta\mathbf{x}_k^{\mathrm{IRC}} = \mathbf{x}_{k+1} - \mathbf{x}_k = -s\mathbf{g}_k/|\mathbf{g}_k|, \tag{2}$$

where s is the step size. Unless very small steps are taken, this approach tends to oscillate about the true IRC. Equation (2) is the simple Euler method for integrating Eq. (1). More sophisticated numerical methods such as a predictor–corrector algorithm can also be used to integrate Eq. (1) and produce improved reaction paths.[8,9] However, a comparison of several methods indicates that even with small step sizes some predictor–corrector methods can lead to severe oscillations of the reaction path in certain regions of energy surfaces.[9]

Ishida, Morokuma, and Komornicki (IMK)[4,5] have improved on Eq. (2) by adding a corrector step in the form of a one-dimensional search. As shown in Fig. 1, a step of length s is taken along $-\mathbf{g}_k$ resulting in a point $\mathbf{x}_{k+1}^*$ with gradient $\mathbf{g}_{k+1}^*$; then $\mathbf{x}_{k+1}$ is obtained by finding the minimum along $\mathbf{d}_k$, the bisector of $-\mathbf{g}_k$ and $\mathbf{g}_{k+1}^*$. A refinement by Schmidt, Gordon, and Dupuis[5] reduces the amount of work needed for the minimization. Both of these can be considered specialized forms of the Euler stabilization method

[a)] Camile and Henry Dreyfus Scholar.

 0021-9606/89/042154-08$02.10

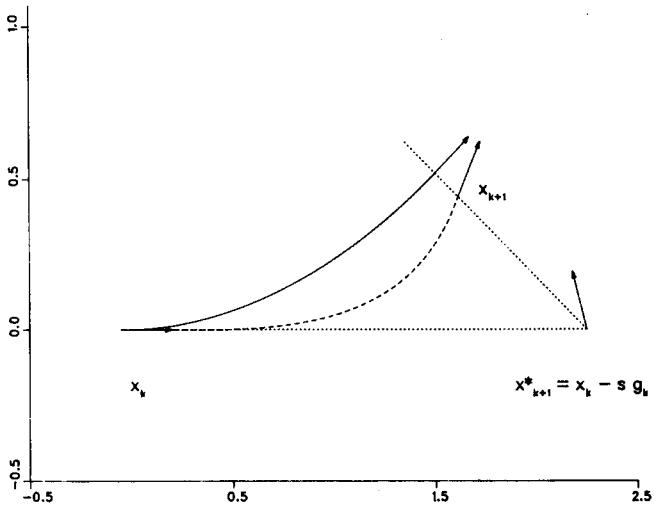

FIG. 1. Reaction path-following algorithm proposed by Ishida, Morokuma, and Komornicki [true path (full curve), approximate path (dashed curve), vectors point downhill, indicating the orientation of $-g$]. From x_k, a point on the reaction path, a step is taken along $-g_k$, yielding position x^*_{k+1} with gradient g^*_{k+1}. Minimization from x^*_{k+1} along the direction of the bisector $d_k = g^*_{k+1}/|g^*_{k+1}| - g_k/|g_k|$, results in x_{k+1}, the approximation to the next point on the reaction path.

for integrating differential equations. Nevertheless, the step size must still be relatively small and numerous points along the reaction path must be calculated for a satisfactory determination of the IRC.[4,5,9]

Müller and Brown[6] have devised a method that can tolerate larger step sizes, as shown in Fig. 2. A step of fixed length s is taken and the direction is chosen so as to minimize the energy with respect to the remaining degrees of freedom. For a molecule with N degrees of freedom, a constrained $N-1$ dimensional minimization is required on the surface of a hypersphere of radius s. Although each step involves an optimization, much larger steps can be taken and the net amount of work is reduced. However, this method tends to estimate the curvature of the reaction path incorrectly, and smaller steps are needed for more curved reaction paths.[6]

Page and McIver[10] have derived general analytical formulas for the reaction path tangent vector and curvature vector in terms of the first, second, and third derivatives of the energy. To use this method to compute a reaction path, the Hessian must be calculated at some points on the path (and some components of the third derivatives at the transition state). Direct evaluation of the higher derivatives (either analytically or numerically) is practical for analytical energy functions, but may be costly for *ab initio* calculations, especially beyond the Hartree–Fock level.

A new reaction path following algorithm is proposed that requires only first derivatives at points along the path (and the transition vector at the transition state). As shown in Fig. 3, the next point on the path, $\mathbf{x}_{k+1}$, is chosen so that the reaction path between $\mathbf{x}_k$ and $\mathbf{x}_{k+1}$ is an arc of a circle and so that the gradients $\mathbf{g}_k$ and $\mathbf{g}_{k+1}$ are tangent to this path. Let the two tangents to the circle intersect at $\mathbf{x}^*_{k+1}$. From simple considerations in planar geometry, it can be shown that $\mathbf{x}_k$, $\mathbf{x}^*_{k+1}$, and $\mathbf{x}_{k+1}$ form an isosceles triangle. The pivot point $\mathbf{x}^*_{k+1}$ is found by first taking a step of length $\frac{1}{2}s$ along the gradient $\mathbf{g}_k$.

$$\mathbf{x}^*_{k+1} = \mathbf{x}_k - 1/2s\mathbf{g}_k/|\mathbf{g}_k|. \tag{3}$$

Note that no calculation is performed at $\mathbf{x}^*_{k+1}$. A constrained minimization is carried out on the surface of a sphere of radius $\frac{1}{2}\cdot s$ and centered at $\mathbf{x}^*_{k+1}$. The result of this minimization is $\mathbf{x}_{k+1}$. Because of the constraint, the residual gradient $\mathbf{g}_{k+1}$ is parallel to $\mathbf{x}_{k+1} - \mathbf{x}^*_{k+1}$. Hence, $\mathbf{x}_k$ and $\mathbf{x}_{k+1}$ lie on an arc of a circle with tangents $\mathbf{g}_k$ and $\mathbf{g}_{k+1}$.

In comparison with various existing methods, the pres-

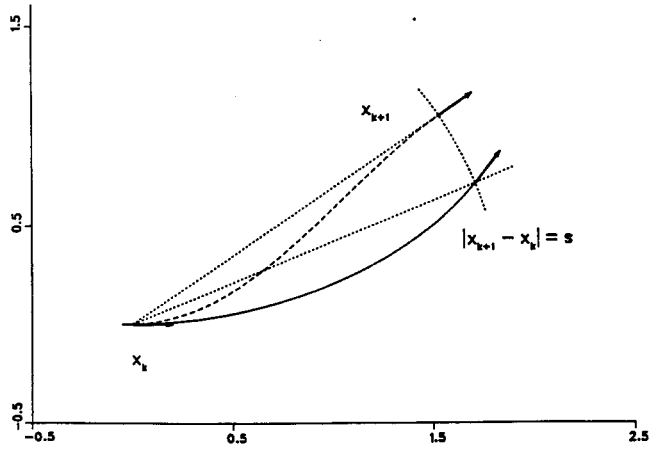

FIG. 2. Reaction path-following algorithm of Müller and Brown [true path (full curve), approximate path (dashed curve), vectors point downhill, indicating the orientation of $-g$]. From x_k, a point on the reaction path, a step of length s is taken along $-g_k$ (the downhill direction). The approximation to the next point on the path x_{k+1} is found by minimizing the energy with the distance $|x_{k+1} - x_k|$ constrained to be s.

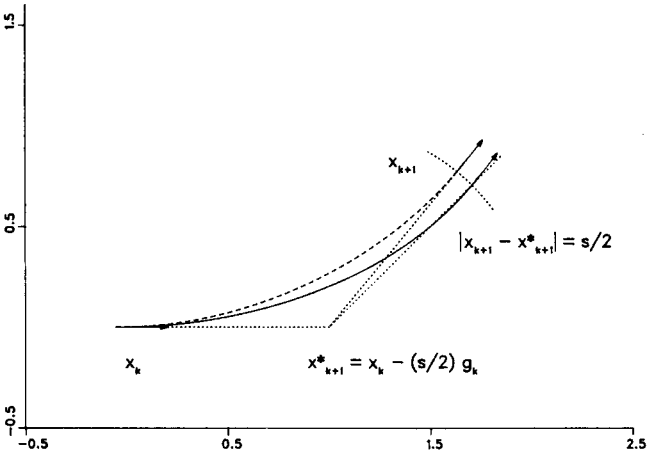

FIG. 3. Reaction path-following algorithm proposed in the present work [true path (full curve), approximate path (dashed curve), vectors point downhill, indicating the orientation of $-g$]. From x_k, a point on the reaction path, a step of length $\frac{1}{2}s$ is taken along $-g_k$ yielding x^*_{k+1} (no energy or gradient calculation at x^*_{k+1}). The approximation to the next point on the path x_{k+1} is found by minimizing the energy with the distance $|x_{k+1} - x^*_{k+1}|$ constrained to be $\frac{1}{2}s$. By construction, the reaction path between x_k and x_{k+1} is an arc of a circle tangent to g_k and g_{k+1}.

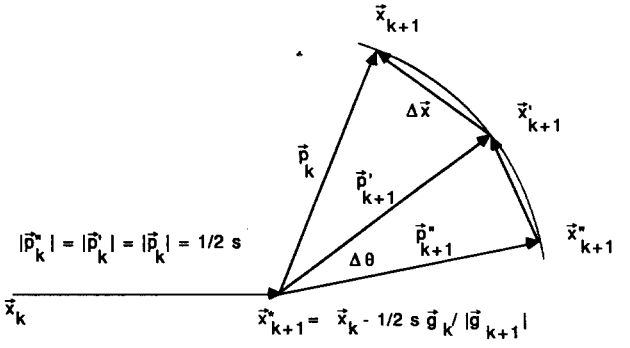

FIG. 4. Definition of vectors used in the present algorithm. The approximation to the new point on the path $\mathbf{x}_{k+1}$ is found by minimizing the energy with the constrain that the magnitude of $\mathbf{p}_{k+1} = \mathbf{p}'_{k+1} + \Delta\mathbf{x} = \mathbf{x}_{k+1} - \mathbf{x}^*_{k+1}$ always equals $\frac{1}{2}s$.

ent algorithm has some similarities and a number of advantages. Like the Müller and Brown method,[6] the present algorithm requires a constrained $N-1$ dimensional optimization. However, numerical tests indicate that larger step sizes can be used in the present algorithm to achieve the same accuracy in reaction path following (e.g., Figs. 5 and 6). As is shown in the Appendix, for an arbitrary point on the reaction path (including the transition state), the present algorithm predicts the correct tangent vector and curvature vector in the limit of small step sizes. Thus, the proposed method qualifies as a second order algorithm (i.e., by the conventional definition of order, the Taylor expansion of the predicted path is correct to s^2). The method devised by Ishida, Morokuma, and Komornicki does not have the correct tangent vector for small step sizes unless the stabilization step is omitted (hence, it is a first order algorithm at best). The Müller–Brown algorithm does use the correct tangent vector but, as demonstrated in the Appendix, results in the wrong curvature in the limit of small step sizes (thus it

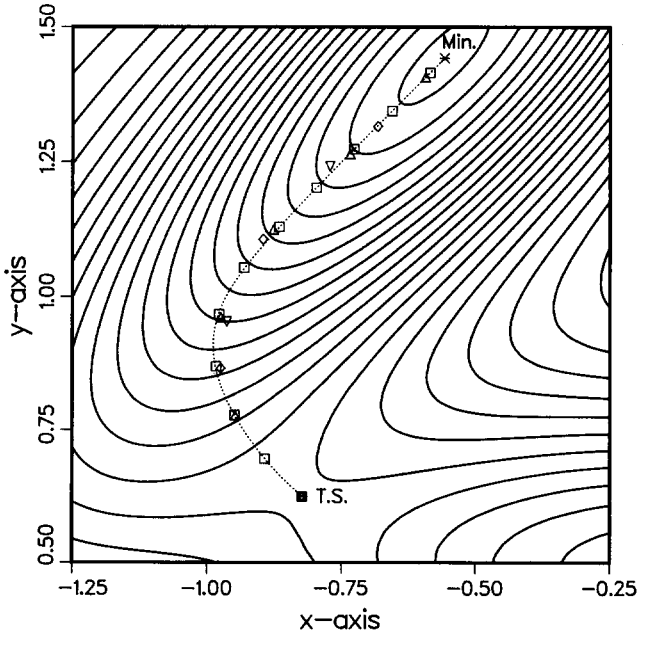

FIG. 5. Reaction paths on a section of the Müller–Brown potential obtained by the present algorithm when step sizes of 0.1 (□), 0.2 (△), 0.3 (◇), and 0.4 (▽) are used. The dotted curve is the true reaction path for this surface.

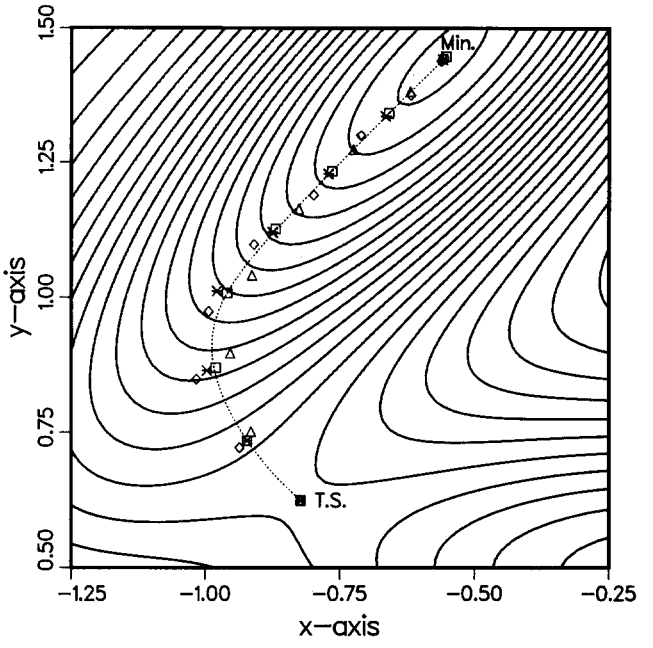

FIG. 6. Reaction paths on the Müller–Brown potential generated by Ishida, Morokuma, and Komornicki algorithm (△), Müller and Brown method (◇), Page and McIver approach (*), and the present algorithm (□) with a step size of 0.15. The dotted curve is the true reaction path for this surface.

is also only a first order method, though potentially more stable than the IMK algorithm since the second order terms are almost correct). The Page and McIver approach is a second order method since it employs the correct tangent and curvature vectors at any point on the reaction path. However, the second derivative matrix is required at several points along the path, whereas the present method uses only first derivatives. Curiously, standard higher order methods for numerical solution of differential equations can be inferior to low order methods (such as IMK), especially in flat regions of the energy surface.[9]

In order to perform a constrained optimization for the present reaction path following algorithm, it is convenient to make use of the Taylor expansion of the energy:

$$E = E' + \mathbf{g}^T\cdot\Delta\mathbf{x} + \tfrac{1}{2}\Delta\mathbf{x}^T\cdot\mathbf{H}\cdot\Delta\mathbf{x} + \cdots, \tag{4}$$

where E' is the energy of a point $\mathbf{x}'_{k+1}$ on the sphere of radius $\frac{1}{2}\cdot s$ centered at $\mathbf{x}_{k+1}$, $\mathbf{g}$ is the gradient and $\mathbf{H}$ is the Hessian. Let $\Delta\mathbf{x}$ be the displacement vector from $\mathbf{x}'_{k+1}$ toward the optimized point $\mathbf{x}_{k+1}$. The following vectors can be defined (see Fig. 4):

$$\mathbf{p}' = \mathbf{x}'_{k+1} - \mathbf{x}^*_{k+1}, \tag{5}$$

$$\Delta\mathbf{x} = \mathbf{x}_{k+1} - \mathbf{x}'_{k+1}, \tag{6}$$

$$\mathbf{p} = \mathbf{p}' + \Delta\mathbf{x} = \mathbf{x}_{k+1} - \mathbf{x}^*_{k+1}. \tag{7}$$

To simplify the notation, the subscript $k+1$ will be omitted. Since the radius of the sphere must be fixed at $\frac{1}{2}\cdot s$, the energy E must be minimized with the constraint

$$\mathbf{p}^T\cdot\mathbf{p} = (\tfrac{1}{2}s)^2. \tag{8}$$

A Lagrange function can be constructed by truncating the Taylor's expansion in Eq. (4) at the quadratic term and making use of the constraint in Eq. (8);

$$L(\lambda) = E' + \mathbf{g}^T \cdot \Delta\mathbf{x} + \tfrac{1}{2}\Delta\mathbf{x}^T \cdot \mathbf{H} \cdot \Delta\mathbf{x} - \tfrac{1}{2}\lambda\,[\mathbf{p}^T \cdot \mathbf{p} - (\tfrac{1}{2}s)^2], \tag{9}$$

where λ is the undetermined multiplier. Since $\partial L(\lambda)/\partial\Delta\mathbf{x}$ and $\partial L(\lambda)/\partial(\lambda)$ must be zero at the minimum (stationary conditions), the following expression for $\Delta\mathbf{x}$ is obtained:

$$\Delta\mathbf{x} = -(\mathbf{H} - \lambda\,\mathbf{I})^{-1} \cdot (\mathbf{g} - \lambda\mathbf{p}'), \tag{10}$$

where $\mathbf{I}$ is the unit matrix. The value of λ must be chosen so that $\mathbf{p} = \mathbf{p}' + \Delta\mathbf{x}$ satisfies Eq. (8), the constraint on the step length. Substitution of Eq. (10) into Eq. (8) yields

$$[\mathbf{p}' - (\mathbf{H} - \lambda\,\mathbf{I})^{-1} \cdot (\mathbf{g} - \lambda\mathbf{p}')]t \cdot [\mathbf{p}' - (\mathbf{H} - \lambda\,\mathbf{I})^{-1} \cdot (\mathbf{g} - \lambda\mathbf{p}')] = (\tfrac{1}{2}s)^2. \tag{11}$$

With a suitable initial guess, this equation can be solved iteratively for λ. To ensure that the reaction path is followed in the descent direction, λ must be less than the lowest eigenvalue of $\mathbf{H}$. Simons *et al.*[11] have outlined a method for determining λ; however, a simple Newton–Raphson root search is sufficient for the present work.

If the predicted displacement, $\Delta\mathbf{x}$ in Eq. (10), or the component of the gradient tangent to the sphere, $\mathbf{g} - (\mathbf{g}^T \cdot \mathbf{p}/|\mathbf{p}|^2)\mathbf{p}$, is larger than the desired cutoff, the process is repeated [Eqs. (4)–(11)]. The stability of the optimization can be improved by preceding the quasi-Newton optimization steps with a one-dimensional search on the surface of the sphere between the current and previous points using polynomial interpolation. Let $\mathbf{x}'$ and $\mathbf{x}''$ be the current and previous points, respectively, in the search for $\mathbf{x}_{k+1}$, the optimized point on the path. Then, the interpolated point $\mathbf{x}^{\text{interp}}$ on the hypersphere and the corresponding gradient $\mathbf{g}^{\text{interp}}$, can be obtained by the following relations:

$$\mathbf{x}^{\text{interp}} = \mathbf{x}^* + \mathbf{p}^{\text{interp}}, \tag{12}$$

$$\mathbf{g}^{\text{interp}} = \mathbf{g}''(1 - \theta/\theta') + \mathbf{g}(\theta/\theta') \tag{13}$$

with

$$\mathbf{p}^{\text{interp}} = \mathbf{p}''[\cos(\theta) - \sin(\theta)\cos(\theta')/\sin(\theta')] + \mathbf{p}'[\sin(\theta)/\sin(\theta')], \tag{14}$$

$$\theta = g''(\text{per})\theta'/[g''(\text{per}) - g'(\text{per})], \tag{15}$$

where $g'(\text{per})$ and $g''(\text{per})$ are the components of the gradient perpendicular to $\mathbf{p}'_{k+1}$ and $\mathbf{p}''_{k+1}$ evaluated at $\mathbf{x}'$ and $\mathbf{x}''$, respectively, θ' is the angle between the vectors $\mathbf{p}'_{k+1}$ and $\mathbf{p}''_{k+1}$. The interpolated quantities $\mathbf{x}^{\text{interp}}$ and $\mathbf{g}^{\text{interp}}$ are then used in the quasi-Newton step for the next prediction of $\mathbf{x}_{k+1}$.

The optimizations start with the analytical Hessian at the transition state. At each subsequent step, the Hessian $\mathbf{H}$ is updated by the BFGS[12] formula given by

$$\mathbf{H}' = \mathbf{H}'' + (\Delta\mathbf{g}' \cdot \Delta\mathbf{g}'^t)/(\Delta\mathbf{g}'^t \cdot \Delta\mathbf{x}') - (\mathbf{H}'' \cdot \Delta\mathbf{x}') \cdot (\Delta\mathbf{x}'^T \cdot \mathbf{H}'')/(\Delta\mathbf{x}'^T \cdot \mathbf{H} \cdot \Delta\mathbf{x}'), \tag{16}$$

where $\Delta\mathbf{g}' = \mathbf{g}' - \mathbf{g}''$, $\Delta\mathbf{x}' = \mathbf{x}' - \mathbf{x}''$ and the superscripts $'$ and $''$ refer to the current and previous points, respectively, in the search for $\mathbf{x}_{k+1}$. An advantage of the BFGS method is that the change in the Hessian is positive definite,[13,14] a desirable feature when searching for a minimum. An alternative updating scheme used in gradient searches for minima and transition states[19] is also suitable, and may be preferable if the present algorithm is used to follow valleys and climb toward transition structures.

III. APPLICATIONS

The algorithm described above has been incorporated into the GAUSSIAN 88 system of programs.[15] The model surface and test reactions were chosen to illustrate a variety of reaction types. The reaction paths were calculated in internal coordinates (bond lengths in a.u., angles in radians) without mass weighting.[21] The optimizations were started at the transition state using the analytical Hessian. Unless otherwise stated, the Hessian was obtained by updating.

A. Müller–Brown potential

The method was first tested on the two-dimensional model surface devised by Müller and Brown[6]:

$$E(x,y) = \Sigma_i A_i \exp[a_i(x - x_{0i})^2 + b_i(x - x_{0i}) \cdot (y - y_{0i}) + c_i(y - y_{0i})^2], \tag{17}$$

where A_i, a_i, b_i, c_i, x_{0i}, and y_{0i} are constants given in Ref. 6. This surface has three minima and two saddle points. Calculations were performed for the reaction path with the largest curvature: from the saddle point located at $(-0.822, 0.624)$ to the minimum located at $(-0.558, 1.442)$. Step sizes of 0.1, 0.2, 0.3, and 0.4 were used and all gradients and Hessians were calculated analytically. Figure 5 shows the points along the reaction path obtained with different step sizes. The points obtained with step sizes ranging from 0.1 to 0.4 lie on nearly the same path. When the step is larger than the radius of curvature of the path, some degradation is seen.

The Ishida, Morokuma, and Komornicki (IMK) method,[4] the Müller–Brown (MB) approach,[6] the Page and McIver algorithm,[9] and the present method are compared to the correct reaction path in Figs. 6 and 7. For each algorithm, a step size equal to 0.15 is used. The IMK method overshoots the bend in the path, while the MB algorithm cuts the corner (Fig. 6). The Page and McIver method and the present algorithm follow the path much more closely. Reaction path curvature is a very sensitive indicator of the performance of a reaction path following algorithm. Figure 7 compares the curvatures [computed with Eq. (A4)[9]] for the points on the four different paths in Fig. 6. For this step size (0.15), the present method is clearly superior to IMK and MB. Beyond the peak in the curvature, the present algorithm is even somewhat better than the Page and McIver method. To achieve a similar behavior in following the path and reproducing the curvature, the step sizes for the IMK and MB methods need to be reduced by a factor of at least 10.

B. HCN→HNC isomerization

This reaction has been used frequently to test transition state optimization methods and reaction path algorithms (e.g., Refs. 6 and 9). *Ab initio* calculations were carried out at the Hartree–Fock level with minimal basis set (STO-3G). The reaction path was followed from the transition state ($R_{\text{C-N}} = 1.222$ Å, $R_{\text{C-H}} = 1.202$ Å, ∠HCN angle = 72.8°) to the reactants ($R_{\text{C-N}} = 1.15$ Å, $R_{\text{C-H}} = 1.07$ Å) and to the products ($R_{\text{C-N}} = 1.17$ Å, $R_{\text{C-H}} = 1.01$ Å) using step sizes

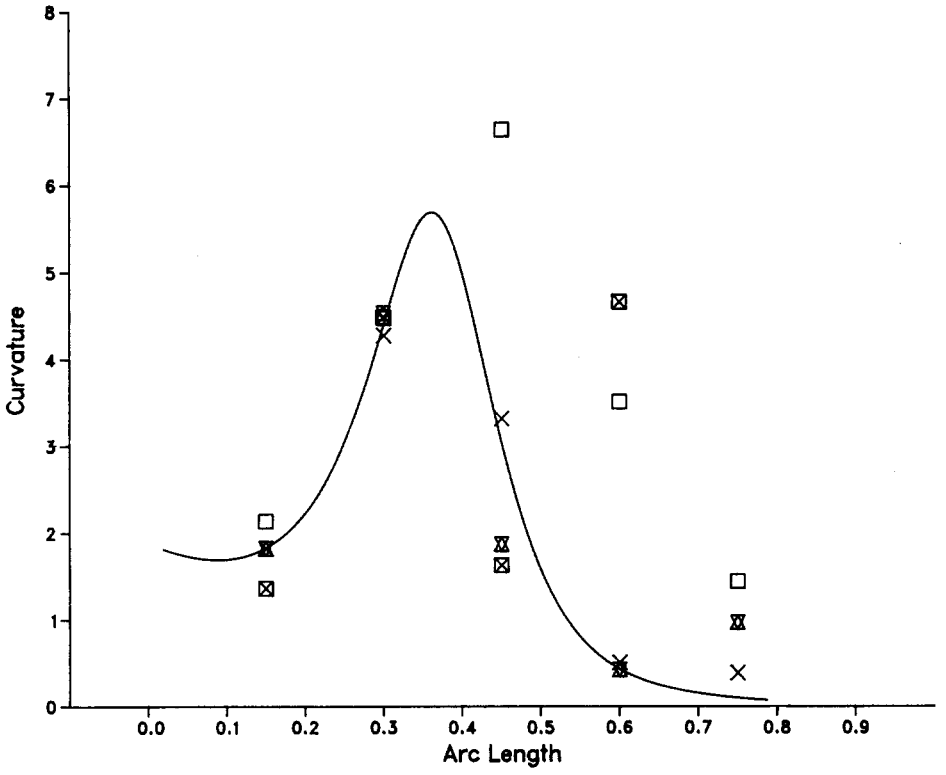

FIG. 7: Curvatures for the reaction paths on the Müller–Brown surface in Fig. 6: Ishida, Morokuma, and Komornicki algorithm (⊠), Müller–Brown method (□), Page and McIver approach (XX), and the present algorithm (×) with a step size of 0.15. The solid line is the curvature along the true reaction path.

of 0.1, 0.2, 0.3, and 0.4 a.u. An average of three energy and gradient evaluations were necessary to optimize each point along the reaction path. The resulting isomerization paths are shown in Fig. 8 and agree with the reaction paths obtained by other methods.[4,6,9] Even with a step size of $s = 0.4$, the reaction path is almost the same as for $s = 0.1$, but the overall calculational effort is reduced by $\frac{1}{4}$.

C. $SiH_2 + H_2 \rightarrow SiH_4$

This is a prototype of a three center insertion reaction and has been studied extensively, both theoretically and experimentally.[16,17] *Ab initio* calculations were performed at the HF/3-21G level. Reaction paths connecting the transition state with reactants and products were calculated for step sizes of 0.1, 0.2, 0.3, and 0.4 a.u.; an average of three energy and gradient calculations were needed for each point along the path. Figure 9 shows the corresponding energy profiles along the reaction path. The ability of the algorithm to follow insertion reaction paths with relatively large step sizes is demonstrated by the fact that the points obtained with the various different step sizes all lie on the same path.

D. $CH_4 + H \rightarrow CH_3 + H_2$

Abstraction reactions are important processes in combustion.[18] One of the simplest examples is the reaction $CH_4 + H \rightarrow CH_3 + H_2$. Calculations were performed at the HF/3-21G level using step sizes of 0.1, 0.2, 0.3, 0.4, and 0.9. Figure 10 shows the relationship between the C–H and H–H

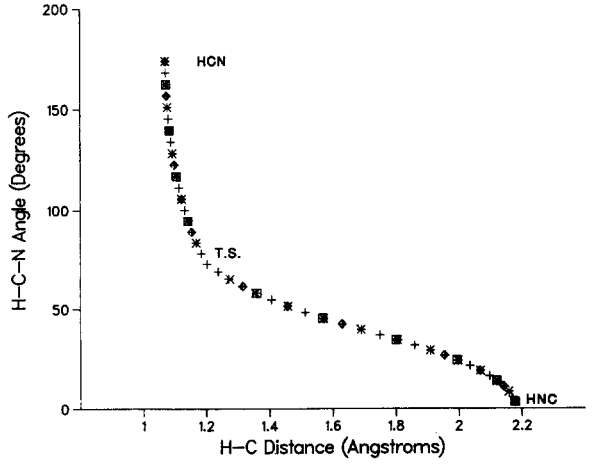

FIG. 8. Reaction path for the H–C–N → H–N–C isomerization at the HF/STO-3G level [step sizes of 0.1 (+), 0.2 (×), 0.3 (◇), and 0.4 (□) a.u. rad].

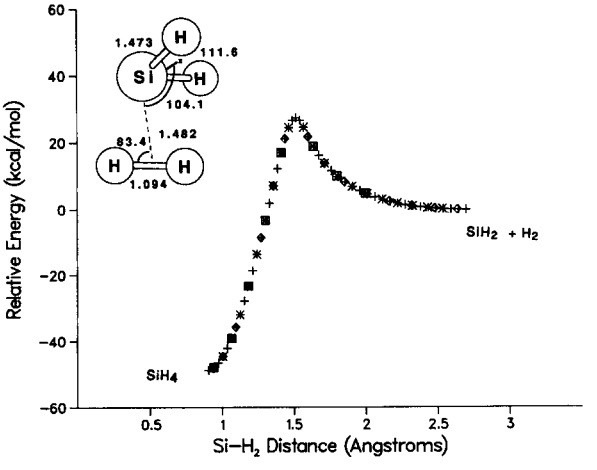

FIG. 9. Energy profile for the reaction $SiH_2 + H_2 \rightarrow SiH_4$ proposed in this work at the HF/3-21G level [step sizes of 0.1 (+), 0.2 (×), 0.3 (◇), and 0.4 (□) a.u. rad].

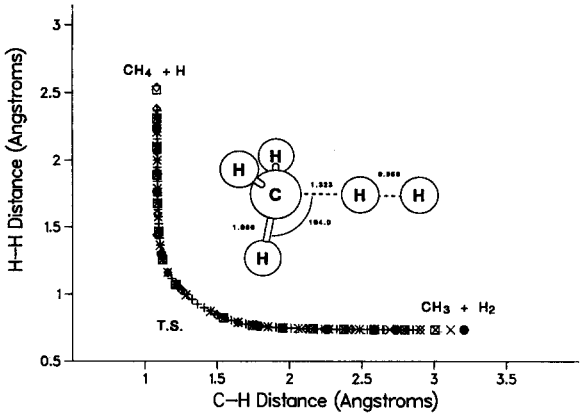

FIG. 10. Reaction path following for $H + CH_4 \rightarrow CH_3 + H_2$ at the HF/3-21G level [step sizes of 0.1 (+), 0.2 (×), 0.3 (◇), and 0.4 (□), and 0.9 (●) a.u. rad].

distances for the different step sizes used. An average of two energy and gradient evaluations per optimized point were necessary to obtain the reaction path for this reaction. The results show how well the reaction path is followed even when large step sizes as large as 0.9 a.u. are used. This is particularly noteworthy in the light of the difficulties that the predictor–corrector methods have with this reaction.[9]

E. $F^- + CH_3F \rightarrow FCH_3 + F^-$

The reaction between fluoride ion and methyl fluoride is a typical example of an S_N2 reaction and constitutes a good test for any reaction path following algorithm. *Ab initio* calculations were performed at the HF/4-31G level and reaction paths were determined for step sizes of 0.1, 0.2, 0.3, and 0.4 a.u. In each optimization process, an average of two energy and gradient calculations were necessary. Figure 11 shows the relationship between the two C–F distances as a function of the distance along the reaction path. The results are similar to the ones obtained by Ishida, Morokuma, and Komornicki for the reaction $H^- + CH_4 \rightarrow CH_4 + H^-$.[4]

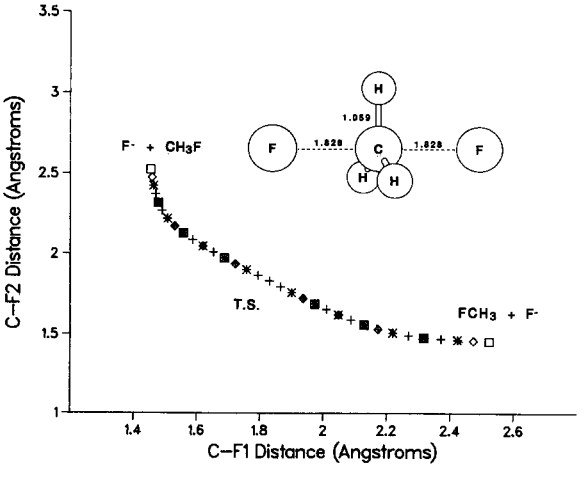

FIG. 11. Reaction path following for the S_N2 reaction $F^- + CH_3F$ at the HF/4-31G level [step sizes of 0.1 (+), 0.2 (×), 0.3 (◇), and 0.4 (□) a.u. rad].

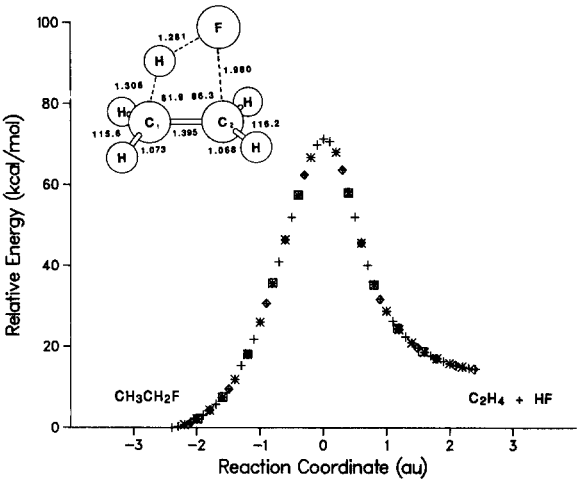

FIG. 12. Potential energy profile for the four-centered elimination process of CH_3CH_2F obtained by the present method [step sizes of 0.1 (+), 0.2 (×), 0.3 (◇), and 0.4 (□) a.u. rad]. The geometry of the transition structure (optimized at the HF/4-31G level) is also shown.

F. $CH_3CH_2F \rightarrow CH_2CH_2 + HF$

This reaction, studied extensively by Kato and Morokuma,[20] is a typical example of a four-centered elimination process. *Ab initio* calculations were carried out at the HF/4-31G level using step lengths of 0.1, 0.2, 0.3, and 0.4 a.u. For each point obtained along the path, an average of two gradient and energy calculations were required. The potential energy as a function of the reaction coordinate is shown in Fig. 12, while Fig. 13 shows the relationship between the H–F distance and the distance between the fluorine atom and the center of mass of the ethylene molecule (RCM). The same reaction path is obtained by all four steps sizes.

IV. CONCLUSIONS

An efficient and reliable algorithm has been developed that can follow reaction paths connecting the transition state with the reactants and products using energy gradients. For an arbitrary point on the path (including the transition state), and in the limit of small step size, the algorithm is

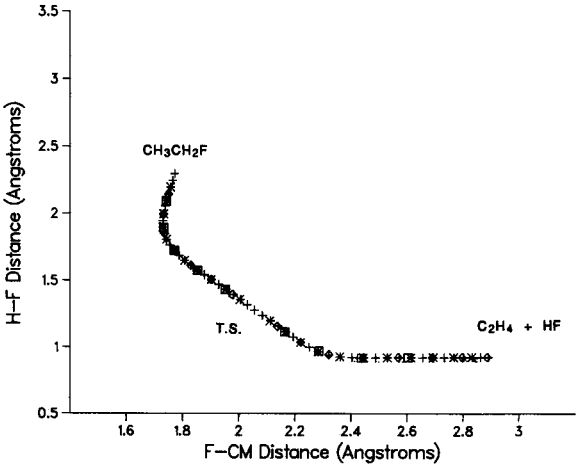

FIG. 13. H–F distance as a function of the distance F–CM between the fluorine atom and the center of mass of ethylene for the reaction shown on Fig. 11 [step sizes of 0.1 (+), 0.2 (×), 0.3 (◇), and 0.4 (□) a.u. rad].

shown to produce a step with the correct curvature vector, whereas the Ishida–Morokuma–Komornicki and Müller–Brown methods do not yield the right values. Test calculations, performed on a model surface and five different kinds of reactions, have shown that the algorithm is stable and efficient even when step lengths are as large as 0.4 a.u. Further studies are in progress comparing the present method with additional algorithms (e.g., predictor corrector methods,[9] Page and McIver[10]), with an emphasis on the curvature computed for points on the path as well as factors affecting the stability of the path following algorithm.

ACKNOWLEDGMENT

This work was supported by a grant from the National Science Foundation (CHE87-11901).

APPENDIX: CURVATURE VECTOR FOR THE PRESENT ALGORITHM IN THE LIMIT OF SMALL STEP SIZE

The general formulas for the curvature vector $\nu^{(1)}$ have been given by Page and McIver.[10] In the notation of Ref. 10, the tangent to the reaction path is

$$\nu = \partial \mathbf{x}/\partial s = -\mathbf{g}/\sqrt{\mathbf{g}^T\mathbf{g}}. \tag{A1}$$

At that transition state, the gradient is zero and ν is chosen as the eigenvector of the Hessian that has the negative eigenvalue. The curvature vector describes the direction and magnitude of the bending of the reaction path away from a straight line:

$$\nu^{(1)} = \partial^2 \mathbf{x}/\partial s^2 = \partial \nu/\partial s. \tag{A2}$$

The reaction path can then be written as

$$\mathbf{x}(s) = \mathbf{x}(0) + s\nu + \tfrac{1}{2}s^2\nu^{(1)} + \cdots. \tag{A3}$$

Note that the curvature vector is perpendicular to the tangent vector. In terms of the second derivative matrix or Hessian, $\mathbf{H}$, the curvature vector at an arbitrary point on the path is[10]

$$\nu^{(1)} = [\mathbf{H}\nu - (\nu^T\mathbf{H}\nu)\nu]/\sqrt{\mathbf{g}^T\mathbf{g}}. \tag{A4}$$

At the transition state, the gradient is zero and the curvature vector depends on $F^{(1)}$, the third derivative matrix projected onto the reaction path, i.e., $F^{(1)}_{ij} = \Sigma_k \partial^3 E/\partial x_i \partial x_j \partial x_k \nu_k$.[10]

$$\nu^{(1)} = [2(\nu^T\mathbf{H}\nu)\mathbf{I} - \mathbf{H}]^{-1}[F^{(1)}\nu - (\nu^T F^{(1)}\nu)\nu]. \tag{A5}$$

The curvature vector for the present algorithm can be determined in the limit of small step size. For a step of size s, the next point on the reaction path is found by moving $\frac{1}{2}s$ along the tangent vector to the pivot point $\mathbf{x}^*_{k+1}$,

$$\mathbf{x}^*_{k+1} = \mathbf{x}_k + \tfrac{1}{2}s\nu, \tag{A6}$$

followed by a step of length $\frac{1}{2}s$ from the pivot point to $\mathbf{x}_{k+1}$

$$\mathbf{x}_{k+1} = \mathbf{x}^*_{k+1} + \{\tfrac{1}{2}s - \mathbf{a}^T\nu + [(\mathbf{a}^T\nu)^2 - (\mathbf{a}^T\mathbf{a})]/s\}\nu + \mathbf{a}. \tag{A7}$$

The vector $\mathbf{a}$ is chosen to minimize the energy. Note that $|\mathbf{x}_{k+1} + \mathbf{x}_k| = \frac{1}{2}s$ correct to second order in s and in $\mathbf{a}$. The overall step is given by

$$\mathbf{x}_{k+1} = \mathbf{x}_k + \{s - \mathbf{a}^T\nu + [(\mathbf{a}^T\nu)^2 - (\mathbf{a}^T\mathbf{a})]/s\}\nu + \mathbf{a}. \tag{A8}$$

The corresponding step in the Müller–Brown approach[6] is

$$\mathbf{x}_{k+1} = \mathbf{x}_k + \{s - \mathbf{a}^T\nu + [(\mathbf{a}^T\nu)^2 - (\mathbf{a}^T\mathbf{a})]/2s\}\nu + \mathbf{a}. \tag{A9}$$

For small s, the vector $\mathbf{a}$ that minimizes the energy can be determined by a single Newton–Raphson step

$$dE/d\mathbf{a} = 0 = dE/d\mathbf{a}|_0 + d^2E/d\mathbf{a}^2|_0\mathbf{a}, \tag{A10}$$

$$\mathbf{a} = -[d^2E/d\mathbf{a}^2|_0]^{-1}[dE/d\mathbf{a}|_0]. \tag{A11}$$

In the limit $s \to 0$, it is sufficient to retain only the lowest order terms in s that are not zero. The derivatives with respect to $\mathbf{a}$ can be written in terms of the derivatives with respect to $\mathbf{x}$ evaluated at $\mathbf{x}_k$.

$$E = E_0 + \mathbf{g}_0{}^T\mathbf{x} + \tfrac{1}{2}\mathbf{x}^T H_0\mathbf{x} + \cdots, \tag{A12}$$

$$dE/d\mathbf{a} = dE/d\mathbf{x}|_0[d\mathbf{x}/d\mathbf{a}] + d^2E/d\mathbf{x}^2|_0[d\mathbf{x}/d\mathbf{a}]\mathbf{x} + \tfrac{1}{2}d^3E/d\mathbf{x}^3|_0[d\mathbf{x}/d\mathbf{a}]\mathbf{x}^2 + \cdots, \tag{A13}$$

$$d^2E/d\mathbf{a}^2 = dE/d\mathbf{x}|_0[d^2\mathbf{x}/d\mathbf{a}^2] + d^2E/d\mathbf{x}^2|_0\{[d^2\mathbf{x}/d\mathbf{a}^2]\mathbf{x} + [d\mathbf{x}/d\mathbf{a}]^2\} + \cdots. \tag{A14}$$

The derivatives of the components of $\mathbf{x}$ with respect to the components of $\mathbf{a}$, evaluated at $\mathbf{a} = 0$ are

$$\partial x_i/\partial a_j = \delta_{ij} - \nu_i\nu_j, \tag{A15}$$

$$\partial^2 x_i/\partial a_j \partial a_k = 2\nu_i(\nu_j\nu_k - \delta_{jk})/s. \tag{A16}$$

When Eqs. (A15) and (A16) are inserted into Eqs. (A13) and (A14), the expressions for the first and second derivatives of the energy with respect to $\mathbf{a}$ can be simplified to

$$\partial E/\partial a_i|_0 = [g_i - (\mathbf{g}^T\nu)\nu_i] + s[\Sigma_j H_{ij}\nu_j - (\nu^T H\nu)\nu_i] + \tfrac{1}{2}s^2[\Sigma_{jk}F_{ijk}\nu_j\nu_k - (\Sigma_{jkl}F_{jkl}\nu_j\nu_k\nu_l)\nu_i] + \cdots, \tag{A17}$$

$$\partial^2 E/\partial a_i \partial a_j|_0 = -2(\mathbf{g}^T\nu)(\delta_{ij} - \nu_i\nu_j)/s + 2(\nu^T H\nu)(\nu_i\nu_j - \delta_{ij}) + [\Sigma_{kl}H_{kl}(\delta_{ik} - \nu_i\nu_k)(\delta_{jl} - \nu_j\nu_l)] + \cdots. \tag{A18}$$

In the limit $s \to 0$, it is sufficient to retain only the lowest order terms in s that are not zero. For an arbitrary point on the reaction path, the first nonzero term in Eq. (A17) is of order s, since $[\mathbf{g} - (\mathbf{g}^T\nu)\nu]$ is zero by the definition of ν in Eq. (A1). The leading term in Eq. (A18) is of order $1/s$. For the limit $s \to 0$, it is sufficient to use only the leading terms in Eqs. (A17) and (A18) to substitute into Eq. (A10):

$$0 = s[\Sigma_j H_{ij}\nu_j - (\nu^T H\nu)\nu_i] - 2(\mathbf{g}^T\nu)[a_i - (\mathbf{a}^T\nu)\nu_i]/s, \tag{A19}$$

$$[a_i - (\mathbf{a}^T\nu)\nu_i] = \tfrac{1}{2}s^2[\Sigma_j H_{ij}\nu_j - (\nu^T H\nu)\nu_i]/(\mathbf{g}^T\nu). \tag{A20}$$

Converting back to vector notation and substitution of $(\mathbf{g}^T\nu) = \sqrt{\mathbf{g}^T\mathbf{g}}$ [obtained from Eq. (A1)] gives

$$[\mathbf{a} - (\mathbf{a}^T\nu)\nu] = \tfrac{1}{2}s^2[H\nu - (\nu^T H\nu)\nu]/\sqrt{\mathbf{g}^T\mathbf{g}}. \tag{A21}$$

Finally, substitution into Eq. (A8) and retention of terms up to order s^2 gives the following expression for the reaction path with the present algorithm in the limit $s \to 0$.

$$x_{k+1} = \mathbf{x}_k + s\boldsymbol{\nu} + \tfrac{1}{2}s^2[H\boldsymbol{\nu} - (\boldsymbol{\nu}^T H\boldsymbol{\nu})\boldsymbol{\nu}]/\sqrt{\mathbf{g}^T\mathbf{g}} + \cdots. \quad \text{(A22)}$$

Comparison with Eqs. (A3) and (A4) reveals that the present algorithm yields the correct curvature vector along with the correct tangent vector.

Corresponding manipulations starting with Eq. (A9) for the Müller–Brown approach[6] result in Eq. (A23), which has the correct tangent vector but has a curvature vector that is too large by a factor of 2.

$$\mathbf{x}_{k+1} = x_k + s\boldsymbol{\nu} + s^2[H\boldsymbol{\nu} - (\boldsymbol{\nu}^T H\boldsymbol{\nu})\boldsymbol{\nu}]/\sqrt{\mathbf{g}^T\mathbf{g}} + \cdots. \quad \text{(A23)}$$

A similar approach can be used to show that the IMK method[4,5] produces neither the correct tangent vector nor the correct curvature vector for an arbitrary point on the path in the limit $s \to 0$.

The curvature of the path at the transition state requires special consideration. Since $\boldsymbol{\nu}$ is an eigenvector of H with an eigenvalue of $(\boldsymbol{\nu}^T H\boldsymbol{\nu})$ [i.e., $H\boldsymbol{\nu} = (\boldsymbol{\nu}^T H\boldsymbol{\nu})\boldsymbol{\nu}$], the first 2 terms in Eq. (A17) are zero. The first term in Eq. (A18) is also zero because the gradient vanishes at the transition state. Substitution of the leading nonzero terms into Eq. (A10) yields

$$\begin{aligned}
0 &= \tfrac{1}{2}s^2[\Sigma_{jk}F_{ijk}\nu_j\nu_k - (\Sigma_{jkl}F_{jkl}\nu_j\nu_k\nu_l)\nu_i] \\
&\quad + \Sigma_j\{2(\boldsymbol{\nu}^T H\boldsymbol{\nu})(\nu_i\nu_j - \delta_{ij}) \\
&\quad + [\Sigma_{kl}H_{kl}(\delta_{ik} - \nu_i\nu_k)(\delta_{jl} - \nu_j\nu_l)]\}a_j \\
&= \tfrac{1}{2}s^2[\Sigma_{jk}F_{ijk}\nu_j\nu_k - (\Sigma_{jkl}F_{jkl}\nu_j\nu_k\nu_l)\nu_i] \\
&\quad - 2(\boldsymbol{\nu}^T H\boldsymbol{\nu})[a_i - (\mathbf{a}^T\boldsymbol{\nu})\nu_i] \\
&\quad + \{\Sigma_j[H_{ij} - (\boldsymbol{\nu}^T H\boldsymbol{\nu})\nu_i\nu_j]\}[a_j - (\mathbf{a}^T\boldsymbol{\nu})\nu_j] \\
&= \tfrac{1}{2}s^2[\Sigma_{jk}F_{ijk}\nu_j\nu_k - (\Sigma_{jkl}F_{jkl}\nu_j\nu_k\nu_l)\nu_i] \\
&\quad - [2(\boldsymbol{\nu}^T H\boldsymbol{\nu})\delta_{ij} - H_{ij}][a_i - (\mathbf{a}^T\boldsymbol{\nu})\nu_i]. \quad \text{(A24)}
\end{aligned}$$

The notation $F_{ij}^{(1)} = \Sigma_k \partial^3 E/\partial x_i \partial x_j \partial x_k\ \nu_k$ [9] and the relation $H\boldsymbol{\nu} = (\boldsymbol{\nu}^T H\boldsymbol{\nu})\boldsymbol{\nu}$ have been used to simplify Eq. (A23). In vector notation expressions for $[\mathbf{a} - (\mathbf{a}^T\boldsymbol{\nu})\boldsymbol{\nu}]$ and for the reaction path are

$$[\mathbf{a} - (\mathbf{a}^T\boldsymbol{\nu})\boldsymbol{\nu}] = \tfrac{1}{2}s^2[2(\boldsymbol{\nu}^T H\boldsymbol{\nu})I - H]^{-1} \times [F^{(1)}\boldsymbol{\nu} - (\boldsymbol{\nu}^T F^{(1)}\boldsymbol{\nu})\boldsymbol{\nu}], \quad \text{(A25)}$$

$$\mathbf{x}_{k+1} = \mathbf{x}_k + s\boldsymbol{\nu} + \tfrac{1}{2}s^2[2(\boldsymbol{\nu}^T H\boldsymbol{\nu})I - H]^{-1} \times [F^{(1)}\boldsymbol{\nu} - (\boldsymbol{\nu}^T F^{(1)}\boldsymbol{\nu})\boldsymbol{\nu}], \quad \text{(A26)}$$

where I is the identity matrix. Comparison with Eq. (A5) shows that the present method yields the correct curvature vector at the transition state. By contrast, the Müller–Brown algorithm[6] gives

$$\mathbf{x}_{k+1} = \mathbf{x}_k + s\boldsymbol{\nu} + \tfrac{1}{2}s^2[(\boldsymbol{\nu}^T H\boldsymbol{\nu})I - H]^{-1} \times [F^{(1)}\boldsymbol{\nu} - (\boldsymbol{\nu}^T F^{(1)}\boldsymbol{\nu})\boldsymbol{\nu}] \quad \text{(A27)}$$

which differs from the correct formula by a factor of 2 in the first term of the denominator.

[1] K. Fukui, Acc. Chem. Res. **14**, 363 (1981).
[2] D. G. Truhlar and B. C. Garret, Acc. Chem. Res. **13**, 440 (1980).
[3] W. H. Miller, N. C. Handy, and J. E. Adams, J. Chem. Phys. **72**, 99 (1980).
[4] K. Ishida, K. Morokuma, and A. Kormornicki, J. Chem. Phys. **66**, 2153 (1977).
[5] M. W. Schmidt, M. S. Gordon, and M. Dupuis, J. Am. Chem. Soc. **107**, 2585 (1985).
[6] K. Müller and L. D. Brown, Theor. Chim. Acta **53**, 75 (1979).
[7] C. P. Baskin, C. F. Bender, C. W. Bauschlicher, Jr., and H. F. Schaefer III, J. Am. Chem. Soc. **96**, 2709 (1974).
[8] W. L. Hase and R. J. Duchovic, J. Chem. Phys. **83**, 3448 (1985).
[9] B. C. Garret, M. J. Redmon, R. Steckler, D. G. Truhlar, K. K. Baldridge, D. Bartol, M. W. Schmidt, and M. S. Gordon, J. Phys. Chem. **92**, 1476 (1988).
[10] M. Page and J. W. McIver, J. Chem. Phys. **88**, 922 (1988).
[11] A. Banerjee, N. Adams, and J. Simons, J. Phys. Chem. **89**, 52 (1985).
[12] C. G. Broyden, J. Inst. Math. Appl. **6**, 76 (1970); R. Fletcher, Comput. J. **13**, 317 (1970); D. Goldfarb, Math. Comput **24**, 23 (1970); D. F. Shanno, *ibid.* **24**, 647 (1970).
[13] L. E. Scales, *Introduction to Non-linear Optimization* (Macmillan, Basingstoke, 1985).
[14] R. Fletcher, *Practical Methods of Optimization* (Wiley–Interscience, New York, 1980), Vol. 1.
[15] M. J. Frisch, M. Head-Gordon, H. B. Schlegel, K. Raghavachari, J. S. Binkley, C. Gonzalez, D. DeFrees, D. J. Fox, R. A. Whiteside, R. Seeger, C. F. Melius, J. Baker, R. Martin, L. R. Kahn, J. J. P. Stewart, E. M. Fluder, S. Topiol, and J. A. Pople, GAUSSIAN 88, Gaussian, Inc., Pittsburgh, PA, 1988.
[16] C. Sosa and H. B. Schlegel, J. Am. Chem. Soc. **106**, 5847 (1984).
[17] P. John and J. H. Purnell, J. Chem. Soc. Faraday Trans. **69**, 1455 (1973).
[18] J. Warnatz, in *Combustion Chemistry*, edited by W. C. Gardiner, Jr. (Springer, New York, 1984), p. 197.
[19] H. B. Schlegel, J. Comp. Chem. **3**, 214 (1982).
[20] S. Kato and K. Morokuma, J. Chem. Phys. **73**, 3900 (1980).
[21] The same procedure can be used to follow the reaction path in mass-weighted coordinates (i.e., the intrinsic reaction path), provided the coordinates, gradients, and Hessians are transformed using the appropriate G matrix (Ref. 22).
[22] M. Sana, G. Reckinger, and G. Leroy, Theor. Chim. Acta **58**, 145 (1981).